

UNIPOLARITY OF THE SOLAR MAGNETIC FIELD IN EQUATORIAL CORONAL HOLES

¹ New Mexico State University, Las Cruces, New Mexico, USA

K. Katuwal, R.T. James McAteer



A study of the unbalanced magnetic polarity distribution of 70 coronal holes was performed. Data from the Helioseismic and Magnetic Imager were used to examine the photospheric line-of-sight magnetic field (B_{LOS}) beneath these coronal holes. The skewness (S) values of the B_{LOS} distributions revealed significant asymmetry, characterized by the dominance of one magnetic polarity, with $\sim 88\%$ of the coronal holes exhibiting a skewness value ranging from $\pm(0.20$ to $0.40)$. The corresponding magnetic flux imbalance (Φ_{imb}) ranges from 20% to 45%. In contrast, quiet-Sun regions show symmetric magnetic field distributions with skewness values less than 0.11 and flux imbalance less than 11.0%. A study of a coronal hole as it traverses across the disk shows that the magnetic field distribution does not evolve significantly over this time, remaining stable across half a solar rotation. A moderate correlation ($r = 0.60$) between the magnetic flux imbalance and the speed of associated HSSs (v_{HSS}) suggests that flux imbalance may contribute to the generation of these faster solar wind streams. These results imply that regions with higher flux imbalance (Φ_{imb}), indicative of more open magnetic field structures, present more favorable conditions for plasma acceleration as compared to closed bipolar field, but the moderate correlation indicates that other factors may also play important roles.



Background:

Coronal Hole:

- In the 1960s, it was observed on X-ray and radio wavelengths, but their true nature was recognized in the 1970s through the Skylab mission.
- Dark regions observed in Extreme Ultraviolet(EUV) and soft X-ray
- Associated with open magnetic field lines
- Low-density and temperature plasma
- Source of the fastest solar wind

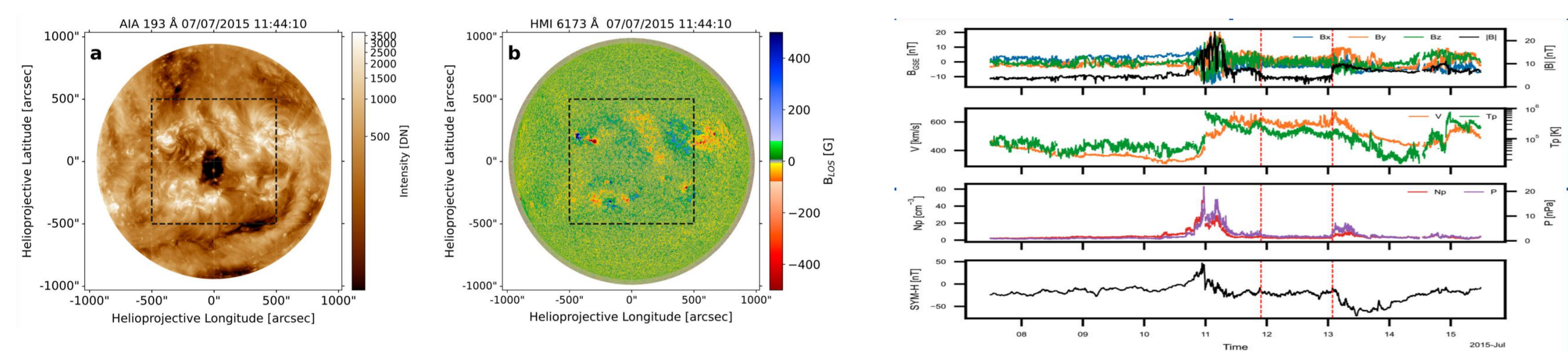


Figure 1. Left: Extreme-ultraviolet image of the solar corona at 193 Å, showing the coronal hole. Right: Corresponding in situ measurements of solar-wind plasma and magnetic-field parameters associated with the coronal-hole source region.

Boundary of Coronal hole

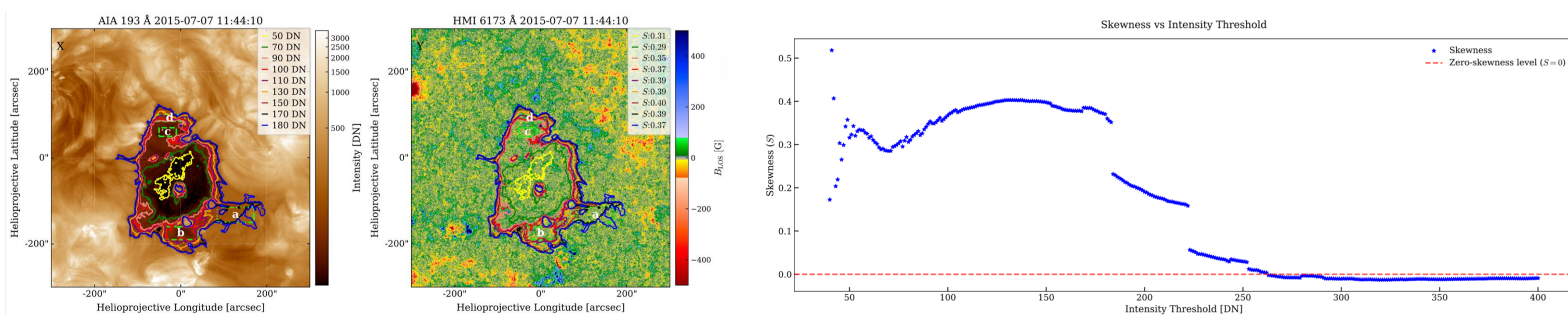


Figure 2. Left: cropped AIA 193 Å image showing coronal-hole boundaries defined by different intensity thresholds. Middle: all boundaries overlaid on the HMI magnetogram. Right: skewness of B_{los} versus intensity threshold; the red dashed line marks $S = 0$.

Distribution of B_{los} inside the Coronal hole

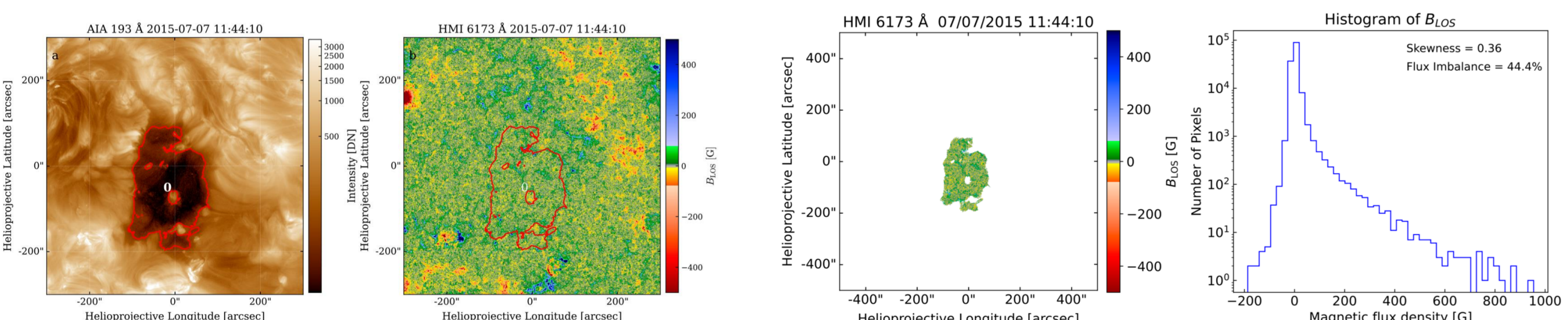


Figure 3. The red contour marks the coronal-hole boundary defined by the 100 DN intensity threshold in the first map. The same contour is overlaid on the photospheric magnetogram in the second panel. The third panel shows the final coronal-hole map after applying the boundary mask. The histogram shows the distribution of the line-of-sight magnetic field, B_{los} , within the Coronal hole.

$$S = \frac{3(\mu - M)}{\sigma}$$

$$\Phi_{imb} = \frac{\sum_{i=1}^N B_i^+ - \sum_{i=1}^N B_i^-}{\left| \sum_{i=1}^N B_i^+ \right| + \left| \sum_{i=1}^N B_i^- \right|} \times 100\%$$

Distribution of B_{los} inside the Quiet Sun

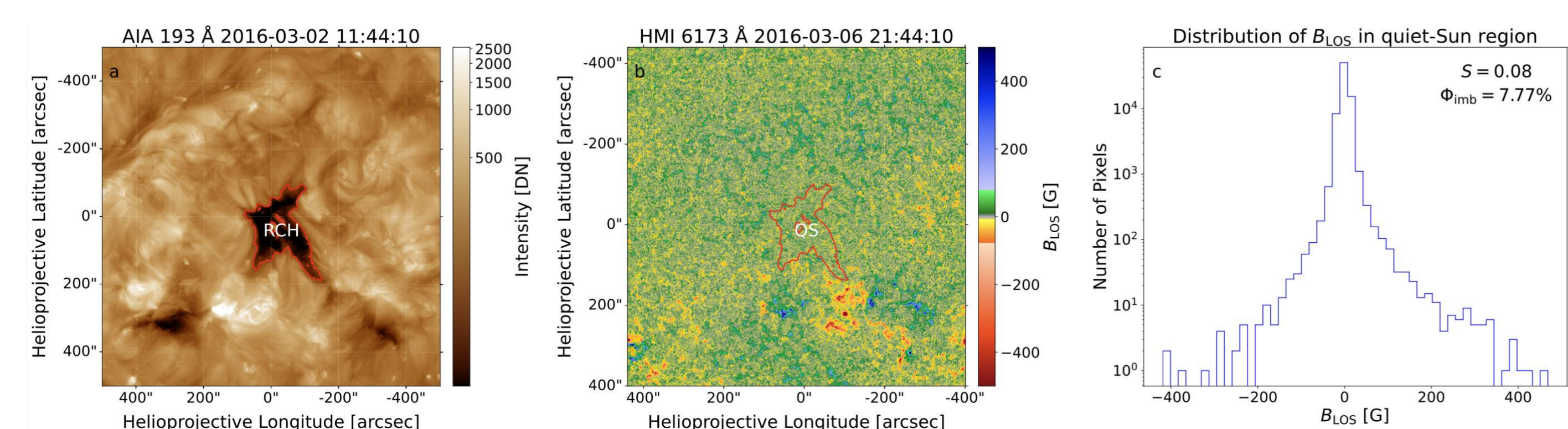


Figure 4. The RCH denotes the reference coronal hole. The red contour in the first panel marks the coronal-hole boundary. A contour of the same size is overlaid on the quiet-Sun (QS) region in the middle panel for comparison. The histogram shows the distribution of B_{los} within the selected QS region.

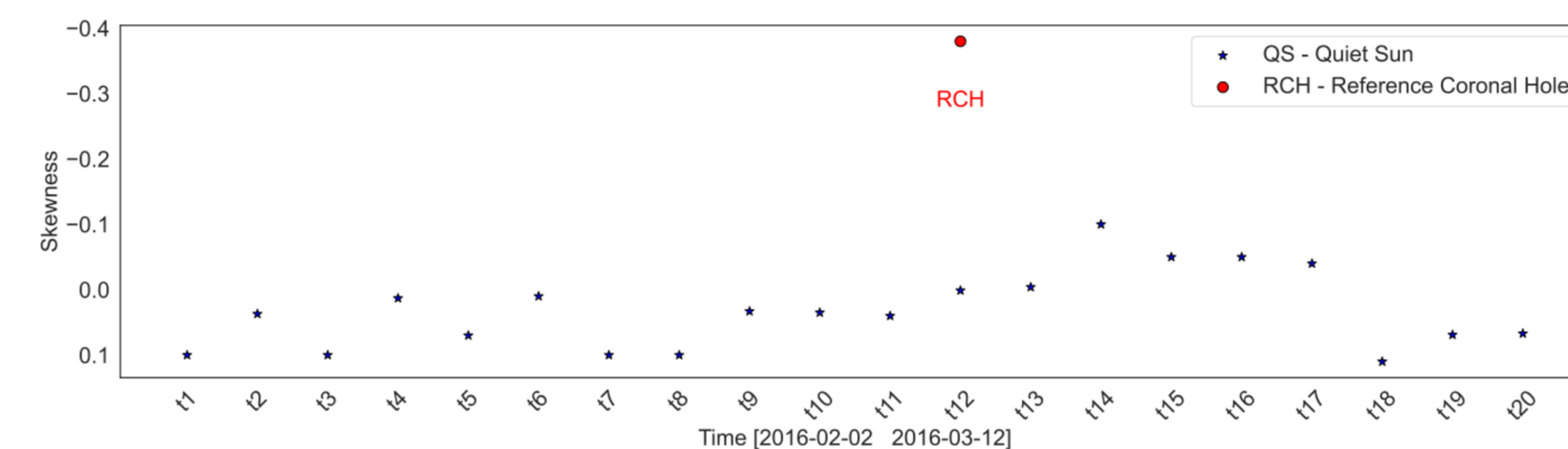


Figure 5. The red circle (RCH) represents the reference coronal hole (same as in Figure 4(a), while the blue star (*) marks the quiet-Sun regions. This plot compares the magnetic field distribution in quiet-Sun regions of equal size to that of the coronal hole (RCH).

Normal Unipolarity in Coronal holes and Quiet Sun regions

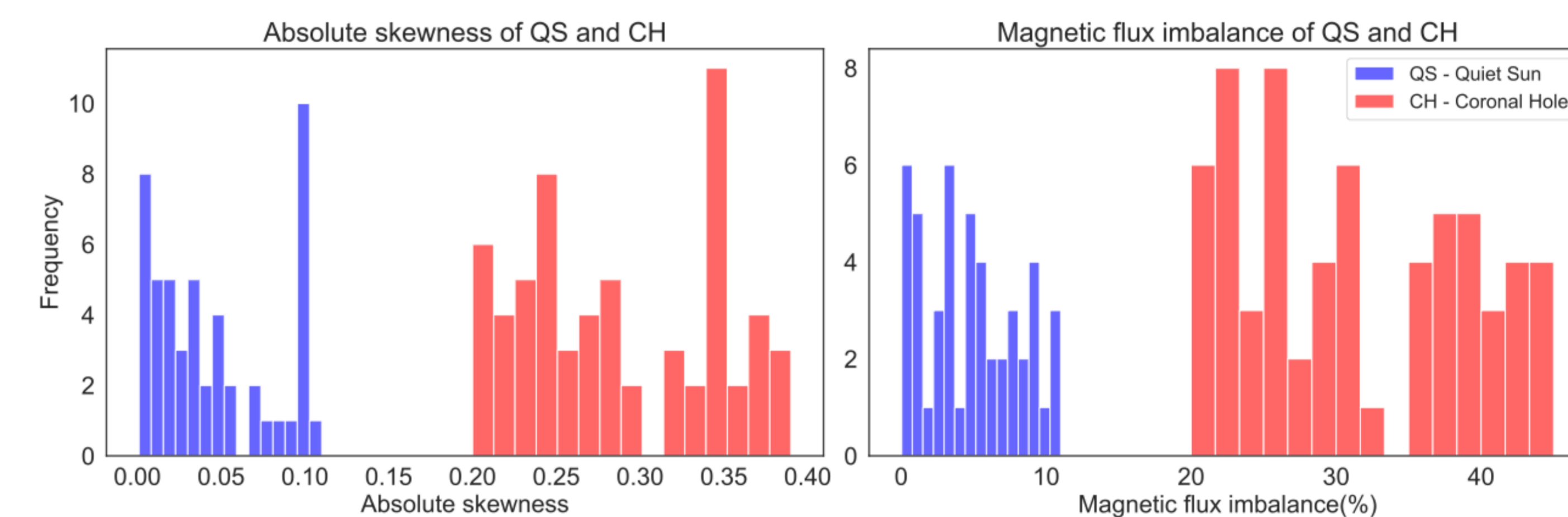


Figure 6. Left: histogram of skewness distribution for the quiet-Sun regions (blue) and coronal holes (red). This graph illustrates how skewness varies between these two solar features. Right: histogram of magnetic flux imbalance for the quiet-Sun regions (blue) and coronal holes (red). This graph shows the differences in magnetic flux imbalance between these regions.

Relationship between magnetic flux imbalance and V_{HSS}

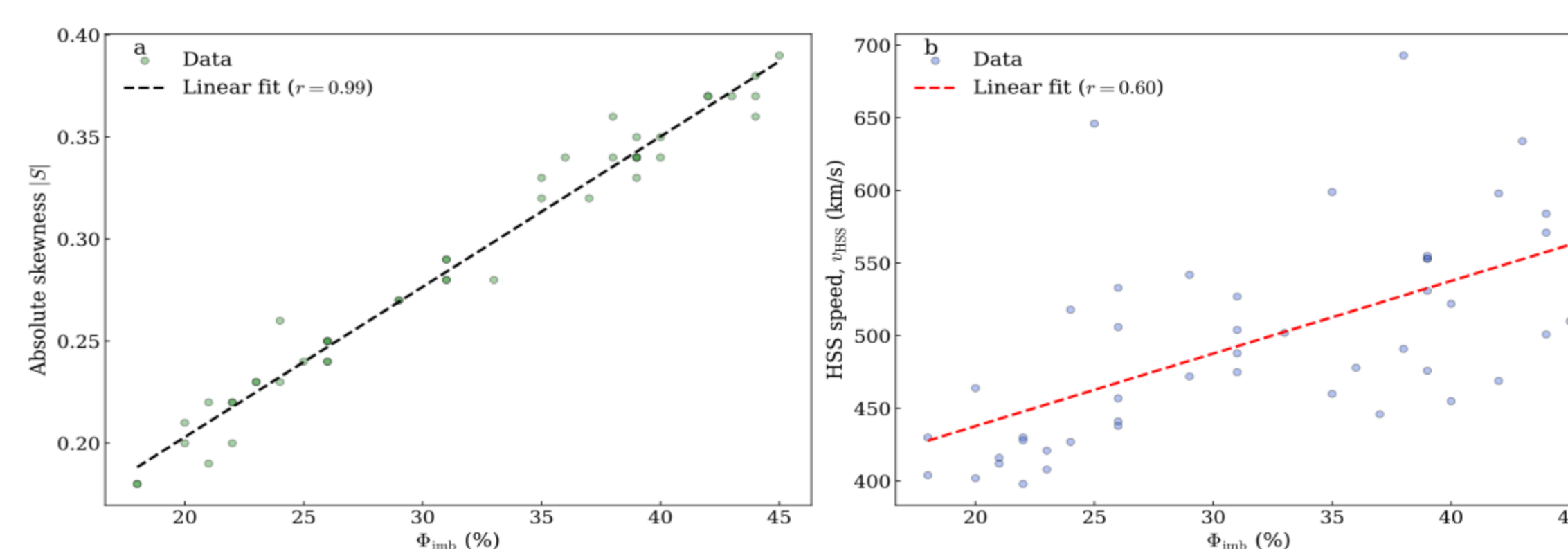


Figure 7. The left panel "a" shows the correlation plot between absolute magnetic skewness and magnetic flux imbalance, while the right panel "b" presents the correlation plot between magnetic flux imbalance and the HSS speed (v_{HSS}) measured at 1 au.

Conclusions

1. The unipolarity of coronal holes in terms of skewness (S) depends on the chosen boundary location, and this can be evaluated by systematically varying an intensity threshold, as illustrated in Figure 2
2. The typical range of magnetic skewness in coronal holes is $\pm(0.20$ to $0.40)$, whereas quiet-Sun regions exhibit values of $\pm(0.001$ to $0.11)$. Similarly, the magnetic flux imbalance in coronal holes ranges from 20% to 45%, compared to 0.037% to 11% in quiet-Sun regions. These distinctions clearly differentiate the B_{LOS} distribution in coronal holes from that in quiet-Sun regions, as shown in Figure 6.
3. We find a moderate Pearson correlation coefficient ($r = 0.60$) between the magnetic flux imbalance and the HSS speed, at 1 au as shown in Figure 7(b), suggesting that flux imbalance is an important factor associated with HSS speed, but its influence is partial, indicating that other physical mechanisms also shape the resulting solar wind stream.

Acknowledge

We gratefully acknowledge travel support from the NMSU College of Arts and Sciences and ASNMSU, which made it possible to present this work

Email: katuwal@nmsu.edu, katuwalnmsu@gmail.com